LA-UR-00-4808

Approved for public release; distribution is unlimited.

Title: SURFACE CHARACTERIZATION OF OXIDATIVE CORROSION OF URANIUM-NIOBIUM ALLOYS

Author(s): Daniel Kelly C1-8
Jennifer A. Lillard MST-6
William L. Manner Union Carbide Corp.
Robert J. Hanrahan, Jr. MST-6
Mark T. Paffett C-18

Submitted to: Journal of Vacuum Science and Technology
(for inclusion in the Proceedings of the American Vacuum Society 2000 Meeting, Boston, October 2000)

Los Alamos
NATIONAL LABORATORY

Los Alamos National Laboratory, an affirmative action/equal opportunity employer, is operated by the University of California for the U.S. Department of Energy under contract W-7405-ENG-36. By acceptance of this article, the publisher recognizes that the U.S. Government retains a nonexclusive, royalty-free license to publish or reproduce the published form of this contribution, or to allow others to do so, for U.S. Government purposes. Los Alamos National Laboratory requests that the publisher identify this article as work performed under the auspices of the U.S. Department of Energy. Los Alamos National Laboratory strongly supports academic freedom and a researcher's right to publish; as an institution, however, the Laboratory does not endorse the viewpoint of a publication or guarantee its technical correctness.

Form 836 (8/00)

DISCLAIMER

This report was prepared as an account of work sponsored by an agency of the United States Government. Neither the United States Government nor any agency thereof, nor any of their employees, make any warranty, express or implied, or assumes any legal liability or responsibility for the accuracy, completeness, or usefulness of any information, apparatus, product, or process disclosed, or represents that its use would not infringe privately owned rights. Reference herein to any specific commercial product, process, or service by trade name, trademark, manufacturer, or otherwise does not necessarily constitute or imply its endorsement, recommendation, or favoring by the United States Government or any agency thereof. The views and opinions of authors expressed herein do not necessarily state or reflect those of the United States Government or any agency thereof.

DISCLAIMER

Portions of this document may be illegible in electronic image products. Images are produced from the best available original document.

Abstract # 515
Program # SS1+MC-ThM9

Surface Characterization of Oxidative Corrosion of U-Nb Alloys

Submitted to: Journal of Vacuum Science and Technology
Proceedings of the 2000 National Conference of the American Vacuum Society

Submitted: September 2000

Dan Kelly[1], Jennifer A. Lillard[2], William L. Manner[3], Robert Hanrahan, Jr.[2], and Mark T. Paffett[1]

1 Chemistry Division, Los Alamos National Laboratory
2 Material Science and Technology Division, Los Alamos National Laboratory
3 Union Carbide Corporation, Charleston, WV

Abstract

We have studied the relative rates of oxidative corrosion of U-Nb alloys containing 2 to 8 wt. % Nb, using X-ray photoelectron spectroscopy (XPS) and depth profiling by sputtered neutrals mass spectroscopy (SNMS). The alloys have been characterized after exposure to dry and humidified air (up to 50% relative humidity) at temperatures from 25 to 125 °C, and after exposure to electrochemical solutions. Oxidation of the U-Nb alloys in a tube furnace results in oxide layers comprised of UO_2 and Nb_2O_5 under all experimental conditions used. The thickness of the oxides increased with treatment time and temperature, but decreased with increasing Nb alloy content. For example, a 48-hour treatment at 75 °C and 50% relative humidity results in an oxide layer on U-2%Nb that is approximately 1.5 times as thick as that on U-8%Nb. Electrochemical oxidation of U-Nb alloys facilely generated $UO_3(\cdot nH_2O)$ and Nb_2O_5 layers ~ 1000 Å thick, qualitatively similar to thermal oxidation results. U-Nb alloys electrochemically oxidized at low pH exhibit oxide layers with near-surface regions (50 Å) enhanced in Nb content, as compared to the bulk material. Surface $UO_3(\cdot nH_2O)$ was not readily reduced upon exposure to molecular D_2; however, D atoms facilely reduced $UO_3(\cdot nH_2O)$ to UO_2.

RECEIVED
OCT 3 1 2000
OSTI

Introduction

In recent years, the need for an effective stockpile stewardship of nuclear materials has led to a fundamental interest in the corrosion behavior of uranium and uranium-base alloys. Uranium metal and uranium alloys readily oxidize when exposed to ambient conditions through interaction not only with oxygen, but also with water vapor, nitrogen, and carbon dioxide. Since the 1940's the corrosion of uranium has been of technological interest, and efforts in the 1950's to alloy uranium with various metals were undertaken in an effort to improve corrosion resistance. Such elements as Nb, Ti, Mo, Zr, and Al have been alloyed with uranium, with varying degrees of success. Additionally, protective coatings such as organic thin films, oxides, and metallic plating have been used atop alloyed uranium surfaces to enhance corrosion resistance. The effectiveness of alloying uranium to protect against corrosion has been discussed in several review articles (**1,2**). "Stainless" uranium alloys, including binary alloys with more than 6 wt. % niobium (with nomenclature U6Nb here) and ternary alloys with 7.5 wt. % Nb and 2.5 wt. % Zr (U7.5Nb2.5Zr), are quite resistant to corrosion under ambient conditions. The density of uranium is reduced by the addition of alloying elements; thus applications requiring high density require a minimal use of alloying material. Most alloying elements are highly soluble in the high temperature γ-phase and minimally soluble in the α-phase of uranium, resulting in metastable microstructure formation. Niobium is completely soluble in the γ-phase of uranium but is less than 0.5 wt. % soluble in the α-phase. The equilibrium structure of U-Nb alloys is therefore a two-phase mixture of Nb rich γ-phase embedded within a matrix of effectively pure α-uranium. Heat treatment of U-Nb alloys minimizes segregation and improves corrosion resistance and mechanical properties.

There are very few studies delineating the mechanism by which alloying elements improve oxidation resistance of uranium. Oxidation of U-Nb and U-Nb-Zr alloys by oxygen or water at 800-1300 K forms multiphase oxide layers consisting of long, narrow, closely spaced Nb-rich stringers embedded within UO_2 (**3, 4**). Large geometrical changes occur during the high temperature oxidation of these alloys. A traditional Wagner-Hauffe oxidation mechanism is likely not applicable to uranium alloys (**5**) at high temperature, since UO_2 exhibits a broad range of stoichiometries; also, for oxide doping effects to be relevant one expects improvement in oxidation resistance with the addition of low levels of alloying elements, which is not observed experimentally. It has been recently shown that (**6**) the formation of a critical density of Nb_2O_5 during the oxidation of U6Nb by O_2 and H_2O is enhances corrosion resistance of U-Nb alloys at temperatures up to 500 K. It was postulated that a thin film of Nb_2O_5 prevents diffusion of reactive anions, such as O^- or OH^-, into the oxide/metal interface region.

In studies of the aging behavior of nuclear materials, one is often interested in the relative behavior of a range of uranium alloys. Here, we report on a corrosion study of U-Nb alloys with Nb content of 2, 4, 6, and 8 wt. %, using x-ray photoelectron spectroscopy (XPS) to determine U and Nb oxidation state, and sputtered neutrals mass spectrometry (SNMS) to determine the relative thicknesses of oxide layers. We have exposed these alloys to thermal and electrochemical oxidation at near-ambient conditions in an effort to ascertain the extent and nature of the corrosion process as a function of Nb content. In all cases, thermal oxidation in humid and dry air at temperatures of 25 to 125 °C leads to the formation of UO_2 and Nb_2O_5 species. At higher temperatures hyperstoichiometric UO_2 forms with increasing exposure time. The thickness of the oxide layers formed during

thermal treatment is dependent upon Nb content, with oxide thickness decreasing with increasing Nb content. Electrochemical oxidation of U-Nb alloys facilely generates $UO_3(\cdot nH_2O)$ and Nb_2O_5 oxide layers. U-Nb alloys electrochemically oxidized at a pH of 4 exhibit oxide layers with near-surface regions (50 Å) enhanced in Nb content as compared to the bulk material. Surface $UO_3(\cdot nH_2O)$ was not readily reduced with room temperature exposure to molecular D_2; however, room temperature D atoms facilely reduced $UO_3(\cdot 2H_2O)$ to UO_2.

Experimental Methods

X-ray photoelectron (XPS) and sputter neutrals mass spectrometry (SNMS) experiments were performed using an ultra-high vacuum (UHV) chamber with a base pressure of approximately 2 x 10^{-10} Torr. The XPS data were obtained using a non-monochromatic MgKα source ($h\nu$ = 1253.6 eV) and the photoemitted electrons were energy sorted by a hemispherical analyzer. Pass energies were 29 eV and incident x-ray power was 250 W. All XP spectra are reported here in terms of binding energy (BE) and instrument calibration was performed in accordance with ASTM procedure (7). The SNMS data were acquired using a differentially pumped 5 keV Xe^+ ion beam passed through a Wein filter and rastered over a 2 x 2 mm area on the sample surface. Depth profiling was performed using an ion beam flux that corresponds to a sputter removal rate of approximately 30 Å/min from thin oxides on uranium (6). All XPS and SNMS data were collected at sample temperatures of approximately 300 K.

Small buttons of the alloys, approximately 4 cm in diameter, were fabricated to ensure homogeneous Nb distribution. The as-cast buttons were solutionized at 800 °C

and then water quenched to room temperature. The U-Nb alloys were mechanically polished using a diamond abrasive to a bright luster prior to oxidation treatments. Impurity levels of the polycrystalline U-Nb alloys were typically 60 ppm C by weight. Alloys were thermally oxidized in a tube furnace using flowing air at controlled temperature and relative humidity. Temperatures of 75 and 125 °C and relative humidities of 0 and 50 % were used for thermal oxidation. Humidified air was generated using a humidity generator (General Eastern) and the relative humidity was measured using a chilled mirror hygrometer (General Eastern). A number of U-Nb samples were treated in the tube furnace simultaneously, and removed at specified time intervals for XPS and SNMS analysis. The UHV chamber is equipped with a multi-platform stage, allowing several samples to be loaded into vacuum and analyzed within a short time period. We note here that oxide growth on samples exposed to ambient conditions during sample transfer to vacuum would be significantly less than oxide growth during thermal treatment.

A Pt tube doser (**8, 9**) was used as a pyrolytic source of deuterium atoms. Briefly, this device consists of a bent Pt tube into which a 0.1 mm diameter hole was drilled. The tube was filled with D_2 and resistively heated to 1300 K to provide the flux of D atoms.

Samples were electrochemically oxidized in a variety of acidic and basic solutions, ranging in pH from 0.5 to 13.6. Samples were held at a potential of +0.6 V_{SCE} (potentials referenced to a saturated calomel electrode, SCE) until the measured current density decreased below 1 $\mu A/cm^2$ (about an hour). All solutions were deaerated with argon before and during the experiment. Working electrodes were made from rectangular pieces (approximately 2 cm x 1 cm) of the U-Nb alloys. Electrical leads were attached to the pieces and the samples were mounted in epoxy with the leads encased in glass rods.

Results and Discussion

Shown in Fig. 1 are U4f, Nb3d, and O1s XP spectra for U4Nb treated at 125 °C and 50 % RH for 60 and 205 hrs. XPS measurements indicate an oxidized uranium surface, with peak energies of ~ 380 and 391 eV for the U $4f_{7/2}$ and $4f_{5/2}$ core levels, indicative of UO_2 formation. XPS also indicates that niobium in the near surface region is oxidized to Nb_2O_5, with peak energies of ~ 207 and 210 eV for the Nb $3d_{5/2}$ and $3d_{3/2}$ core levels. The O1s core level is indicative of oxide formation, with a peak energy of ~ 531 eV. The O1s shoulder at slightly higher binding energy is consistent with the presence of hydroxyl moieties on the surface. This is to be expected since the samples were exposed to ambient conditions after thermal oxidation and prior to placement in the XPS analysis chamber. The U4Nb sample treated for 205 hrs. is comprised of much less hydroxyl, relative to oxide, as expected as a thicker oxide layer has formed with longer treatment time. Quantitative analysis of the XPS results of Fig. 1 indicates that the weight percent of niobium, relative to uranium, in the near surface region is 3.87 %, similar to the stated bulk concentration of 4 % for this sample.

The U 4f core level can be used as an indicator of uranium oxide stoichiometry. A single shakeup peak at 4.5 eV above the main 4f core level, such as that observed (Fig. 1) after 60 hr. oxidation, is indicative of stoichiometric UO_2. With increasing treatment time, uranium in the near surface region is oxidized to hyperstoichiometric UO_{2+x}, indicated by the presence of two shakeup peaks at binding energies of 4 and 5.5 eV above the U $4f_{5/2}$ core level. The transition to hyperstoichiometric oxide was not observed for U2Nb and

uranium in U2Nb remained oxidized as UO_2 with up to 205 hr. thermal treatment at 125 °C and 50 % relative humidity.

Shown in Fig. 2 are intensity curves for U, UO, and Nb obtained during sputtered neutrals mass spectrometry for the samples of Fig. 1. Mass 254 (UO), rather than UO_2, is used as an indicator for the presence of uranium oxide during SNMS based on its higher signal in the mass spectrum. Likewise, SNMS signals corresponding to niobium oxide formation (NbO, Nb_2O_5) are more than an order of magnitude smaller than that for Nb, and hence are not shown. Fig. 2 shows the existence of a thin uranium oxide layer, evident by a decreasing UO signal and increasing U and Nb signals after sputtering approximately 1000 secs. We determine the thickness of oxide layers by first determining a sputter time, denoted as $t_{1/2}$, to achieve a uranium SNMS signal which is half that between initial and final signals, and then convert this to a thickness assuming a sputter rate of 30 Å/min for oxides on U-Nb alloys. For example, considering the left hand panel of Fig. 2, U4Nb treated for 60 hrs. at 125 °C and 50 % has a $t_{1/2}$ of ~ 1200 secs. Increasing treatment time to 205 hr. increases $t_{1/2}$ to 1900 secs. These sputter times correspond to oxide thicknesses of ~ 600 and 950 Å, respectively. In comparison, for U2Nb treated under the same conditions for 60 and 205 hrs. the measured $t_{1/2}$ values are 900 and 2200 secs., corresponding to oxide thicknesses of ~ 750 and 1100 Å, respectively. Not surprisingly, oxide thickness on these uranium alloys is inversely dependent on niobium concentration, since Nb_2O_5 forms a protective layer that is inhibitive to further oxidation.

We note here that all alloy samples analyzed by XPS subsequent to thermal oxidation at temperatures from 25 to 125 °C and relative humidities of 0 and 50 % had

niobium concentrations that were nominally identical (within ~ 0.3 %) to the stated bulk alloy concentration. In fact, XPS of all thermally oxidized U-Nb alloys was qualitatively similar, with uranium forming UO_2-like oxide and niobium forming Nb_2O_5 oxide. Also, SNMS results for all alloys were qualitatively similar to the results of Fig. 2, indicating oxide thicknesses in the range of several hundred Å to greater than 1000 Å for treatment times of several hours to several days, respectively. Generally, at a given temperature and relative humidity, oxide thickness increased with both decreasing niobium concentration and increasing treatment times. Variations in ion sputtering parameters, such as flux, beam current, and detector efficiency, during the analysis of the entirety of samples included here (several months) preclude direct comparison of oxide thickness determined from $t_{1/2}$ values, although qualitative comparisons between sets of data are valid when acquired over short time intervals.

Relative humidity during thermal oxidation has a pronounced effect on the thickness of resulting oxide layers. For example, at 75 °C, a 16 hr. treatment of U4Nb and U6Nb at 50 % relative humidity generates UO_2/Nb_2O_5 oxides that are 4 times thicker than that at 0 % relative humidity (~ 100 vs. 400 Å). The effect of oxidation temperature and treatment time in affecting oxide thickness becomes apparent when comparing U2Nb and U8Nb samples. For example, at temperatures of 75 and 125 °C and 50 % relative humidity, both U2Nb and U8Nb form oxide layers 300 to 350 Å thick in 2 hrs., with the oxide on U2Nb slightly thicker than that on U8Nb. The rate of U8Nb oxidation slows relative to U2Nb such that after 16 hrs. the oxide on U2Nb is ~ 550 Å while that on U8Nb is 350 Å. For this treatment time there is a negligible difference in oxide thickness arising from treatment temperature differences. However, after 48 hrs., oxide thickness on U2Nb

is ~ 600 Å for the 75 °C sample and ~ 750 Å for the 125 °C sample. Comparatively, oxide thickness on U8Nb is 400 Å for the 75 °C sample and ~ 500 Å for the 125 °C sample after 48 hrs.

Prior XPS work involving U-Nb alloys indicates the facile thermal oxidation of uranium to stoichiometric UO_2 (**6**), the U $4f_{7/2}$ core level of which can be well fit by a single peak at 380.0 eV (**10**). Shakeup peaks 6.9 eV higher than the predominant U $4f_{7/2}$ and $4f_{5/2}$ features verify the formation of stoichiometric UO_2. The electrochemically treated U-Nb alloys typically exhibit two peaks in the U $4f_{7/2}$ region, one at a binding energy of 380.0 eV, and another arising at a binding energy of 381.8 eV, which is indicative of $UO_3(\cdot nH_2O)$ formation (**10**). The observance and intensity of the feature at 381.8 eV generally correlates with diminished intensity of shakeup features, as expected for the U(+6) oxidation state.

Fig. 3 shows the U $4f_{7/2}$ XPS peak from U8Nb electrochemically treated at pH 10.7 and +0.6 V_{SCE}. Also shown is the line shape fit of this peak into components corresponding to $UO_3(\cdot nH_2O)$ and UO_2. Line shape fitting was done using two peaks at binding energies 381.8 and 380.0 eV and holding both the full-width at half-maximum (2 eV) and Gaussian/Lorentzian ratio of each peak constant. For this particular sample, line shape fitting provides the distribution of uranium as 90 % $UO_3(\cdot nH_2O)$ and 10 % UO_2.

Table 1 presents results obtained from electrochemically treated samples. Shown is Nb wt. % in the near-surface region and the percentage of uranium as $UO_3(\cdot nH_2O)$. Niobium weight percentage was determined by quantifying U 4f and Nb 3d XPS peak areas using the appropriate sensitivity factors. The percentage of uranium found as $UO_3(\cdot nH_2O)$ was determined using a line shape fitting procedure for the U $4f_{7/2}$ XPS peak,

as described above. All samples of Table 1 were treated at a potential of +0.6 V_{SCE}, and SNMS results indicate that resulting oxide layers were ~ 1000 Å thick.

The addition of niobium in the alloy significantly enhances U passivation and dissolution at acidic pH for all alloys. For example, after treatment at pH 0.5, U4Nb is 86 wt. % Nb in the near-surface region, an approximately 20-fold increase over that of the bulk alloy. Also, at pH 4, the alloys exhibit a 3 to 10 times increase in the Nb wt. % at the surface as compared to the bulk. With increasing pH the enhancement of Nb in the surface region decreases. At pH 7.2, U8Nb has a 10.7 Nb wt. %, only 1.3 times greater than the bulk concentration. At pH 10.7 the surface concentration of Nb is approximately identical to that of the bulk. At pH 13.6, however, uranium in U6Nb is highly passivated and the Nb wt. % in the near surface region is 17.3. Niobium enrichment in the oxide formed upon exposure to acidic solutions results from U dissolution that is thermodynamically favorable at low pH and low U ion concentrations. We suggest that as U dissolves, Nb_2O_5 forms a protective layer allowing a critical concentration of uranium to remain to subsequently form $UO_3(\cdot nH_2O)$.

The samples of Table 1 also exhibit trends in the percentage of uranium extant as $UO_3(\cdot nH_2O)$. In general, the percentage of uranium as $UO_3(\cdot nH_2O)$ increased with increasing pH. This is true for each of the alloys U4Nb, U6Nb, and U8Nb. U2Nb showed the reverse trend, with increasing pH resulting in a decrease in the amount of $UO_3(\cdot nH_2O)$ present. Pourbaix diagrams predict that Nb_2O_5 and $UO_3(\cdot nH_2O)$ should be the only solid oxides formed under electrochemical treatment conditions (for all pH at + 0.6 V_{SCE}) **(11)**. However, all of the mixed oxides of Table 1 show some UO_2 formation. UO_2 is the stable form of uranium oxide in air, and it is possible that during transfer through ambient

conditions from the electrochemical cell to the XPS analysis chamber a reduction of $UO_3(\cdot nH_2O)$ to UO_2 occurred. Air reduction of the oxide may explain the dependence of $UO_3(\cdot nH_2O)$ vs, UO_2 content as well. In all instances, potentiodynamic polarization data suggest $UO_3(\cdot nH_2O)$ formation occurred. It is reasonable to expect that highly protective oxides with greater concentrations of Nb would be the least reduced upon ambient exposure. Also, thicker oxides should reduce less than thinner oxide layers, given identical ambient air exposures. Table 1 indicates that uranium in oxides with high Nb content, for example U8Nb at pH 10.7, was predominantly $UO_3(\cdot nH_2O)$. Oxides with low Nb content showed lesser amounts of $UO_3(\cdot nH_2O)$. We also treated several alloys at a potential of -0.5 V_{SCE} (results not included on table), where UO_2 is the prevalent oxidation state for uranium **(11)**, and found that forcing a two-peak line shape fit of the U $4f_{7/2}$ XPS trace resulted in a determination of 5 to 10 % $UO_3(\cdot nH_2O)$-like character. We interpret this to indicate that line shape fitting of the uranium XPS signal into components ascribed to U(+6) and U(+4) valence states is accurate to within this percentage. Further details, including polarization scans, concerning the electrochemical oxidation of U-Nb alloys will be published elsewhere **(12)**.

Shown in Fig. 4 is the U $4f_{7/2}$ XPS core level trace, as a function of exposure to atomic deuterium at 5×10^{-8} Torr, of U2Nb electrochemically treated at pH 4 and +0.6 V_{SCE}. With increasing D atom exposure, the $UO_3(\cdot nH_2O)$ is reduced toward UO_2. We have peformed the line shape fits to the U $4f_{7/2}$ spectra as described above to determine the ratio of uranium extant as $UO_3(\cdot nH_2O)$ and UO_2. Initially the sample was comprised of 15 % UO_2 and 85 % $UO_3(\cdot nH_2O)$. However, XPS traces after D atom exposure for 30 and 120 min. indicated uranium composition to be 32 and 58 % UO_2-like, respectively. After

exposure to D atoms for 180 min. the uranium was 75 % UO_2. Note that the extent of reduction of $UO_3(\cdot nH_2O)$ is approximately linear with D atom exposure indicating unity reaction probability. Also, the initial U 4f XPS spectrum for this sample was not altered upon exposure to D_2 at 1 x 10^{-7} Torr for 20 min.

Conclusion

The relative oxidative corrosion behavior of U-Nb alloys with 2 to 8 wt. % Nb, exposed to thermal and electrochemical oxidation, has been studied using X-ray photoelectron spectroscopy and sputtered neutrals mass spectrometry. At temperatures from 25 to 125 °C and relative humidity from 0 to 50 %, thermal oxidation leads to the formation of UO_2 and Nb_2O_5 for all alloys. Increasing reaction time serves to increase the likelihood of hyperstoichiometric UO_{2+x} formation, indicated by additional shakeup features in the U 4f XP spectra. SNMS results indicate that oxide thickness resulting from thermal oxidation is nominally several hundred to several thousand Å, and is dependent on treatment temperature, time, and relative humidity, increasing with each parameter. Electrochemically grown oxides consisted of varying amounts of Nb_2O_5, UO_2, and $UO_3(\cdot nH_2O)$. Electrochemically formed $UO_3(\cdot nH_2O)$ was not reduced upon exposure to D_2, but was facilely reduced upon exposure to D atoms.

Figure Captions

Fig. 1. U4f, Nb3d, and O1s photoelectron spectra of U4Nb after treatment for 60 and 205 hrs. at 125 °C and 50 % relative humidity.

Fig. 2. U, Nb, and UO sputtered neutrals signals from U4Nb after treatment for 60 and 205 hrs. at 125 °C and 50 % relative humidity.

Fig. 3. $U4f_{7/2}$ photoelectron peak from U8Nb electrochemically treated at pH 10.7 and +0.6 V_{SCE}. Also shown is the line shape fit of the peak into components ascribed to $UO_3(\cdot nH_2O)$ at 381.8 eV and UO_2 at 380.0 eV.

Fig. 4. $U4f_{7/2}$ photoelectron peak from U2Nb treated at pH 4 and +0.6 V_{SCE}, as a function of exposure to D atoms at 5×10^{-8} Torr.

Table 1. XPS-based results for Nb wt. % in the near-surface region and % UO_3-like character of uranium for a number of electrochemically treated samples.

Sample	pH	Nb. wt. %	UO_3 %
U8Nb	4	22.6	67
U8Nb	7.2	10.7	78
U8Nb	10.7	7.2	90
U6Nb	4	19.9	66
U6Nb	13.6	17.3	95
U4Nb	0.5	86	14
U4Nb	10.7	5.3	80
U2Nb	4	21.5	78
U2Nb	10.7	1.9	32
U	10.7	0	25

References

1. Orman, S., *Phys. Metallurgy of Uranium Alloys*, Burke, J. J., Colling, D. A., and Greenspan, J., Eds., Brook Hill, New York, 1974.

2. L. J. Weirick, *Corrosion of Uranium and Uranium Alloys*, ASM Metals Handbook Vol. 13, ASM, 1988.

3. J. V. Cathcart and C. T. Liu, *Oxid. Met.* **6**, 123 (1973).

4. J. V. Cathcart, R. E. Pawel, and G. F. Petersen, *Oxid. Met.* **3**, 497 (1971).

5. J. V. Cathcart, in: J. Burke, A. David, A. Gorum, *Phys. Metall. Uranium Alloys*, Proc. Army Mater. Technol. Conf., 3rd (1976), Meeting Date 1974, 775-813.

6. W. L. Manner, J. A. Lloyd, R. J. Hanrahan, Jr., and M. T. Paffett, *Appl. Surf. Sci.* **150**, 73 (1999).

7. ASTM Standards on Surface Analysis, American Society for Testing Materials, Philadelphia, PA, 1986.

8. M. R. Voss, H. Busse, and B. E. Koel, *Surf. Sci.* **414**, 330 (1998).

9. T. Engel, K. H. Reider, in: G. Hohler (Ed.), *Structural Studies of Surfaces*, Springer, Berlin, 1982, Vol. 91, p. 55.

10. G. C. Allen, P. M. Tucker, and J. W. Tyler, *J. Phys. Chem.* **86**, 224 (1982).

11. M. Pourbaix, *Atlas of Electrochemical Equilibria*, Houston, TX: NACE (1974).

12. J. A. Lillard, D. Kelly, M. T. Paffet, and R. J. Hanrahan, Jr., submitted, *J. Electrochem. Soc.*

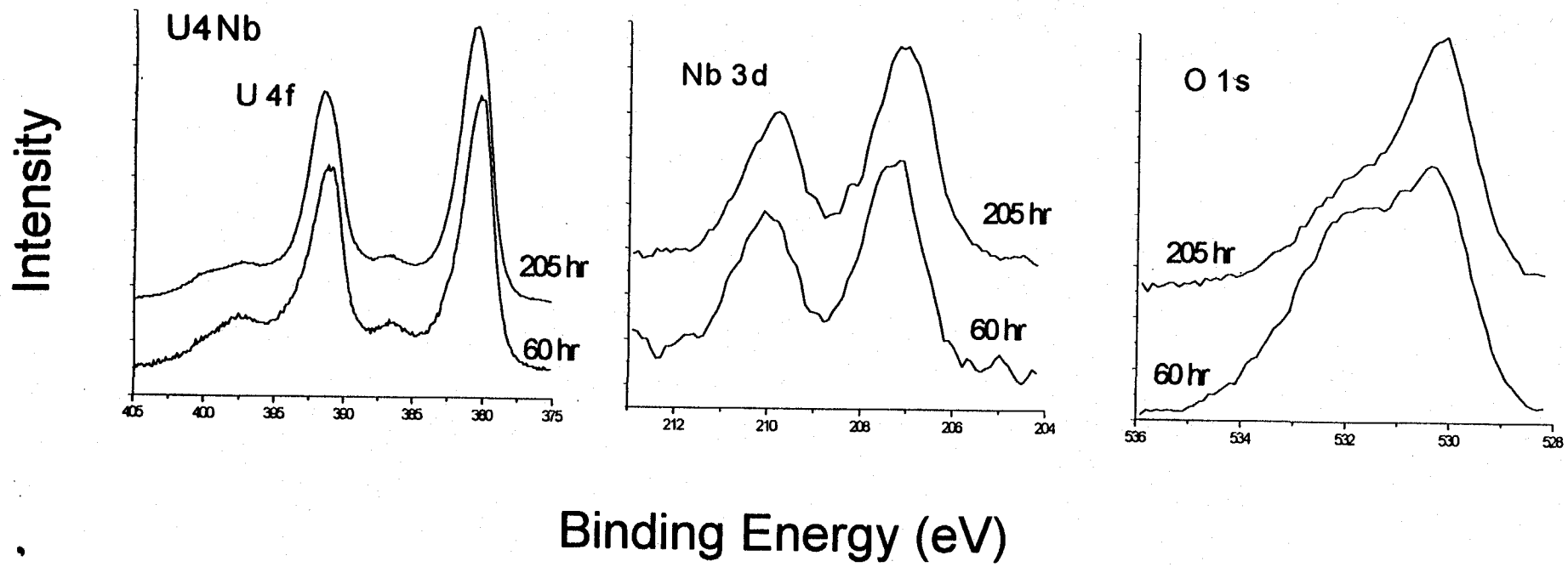
U4Nb
U 4f
205 hr
60 hr
405
400
395
390
385
380
375
Nb 3d
205 hr
60 hr
212
210
208
206
204
O 1s
205 hr
60 hr
536
534
532
530
528
Intensity
Binding Energy (eV)

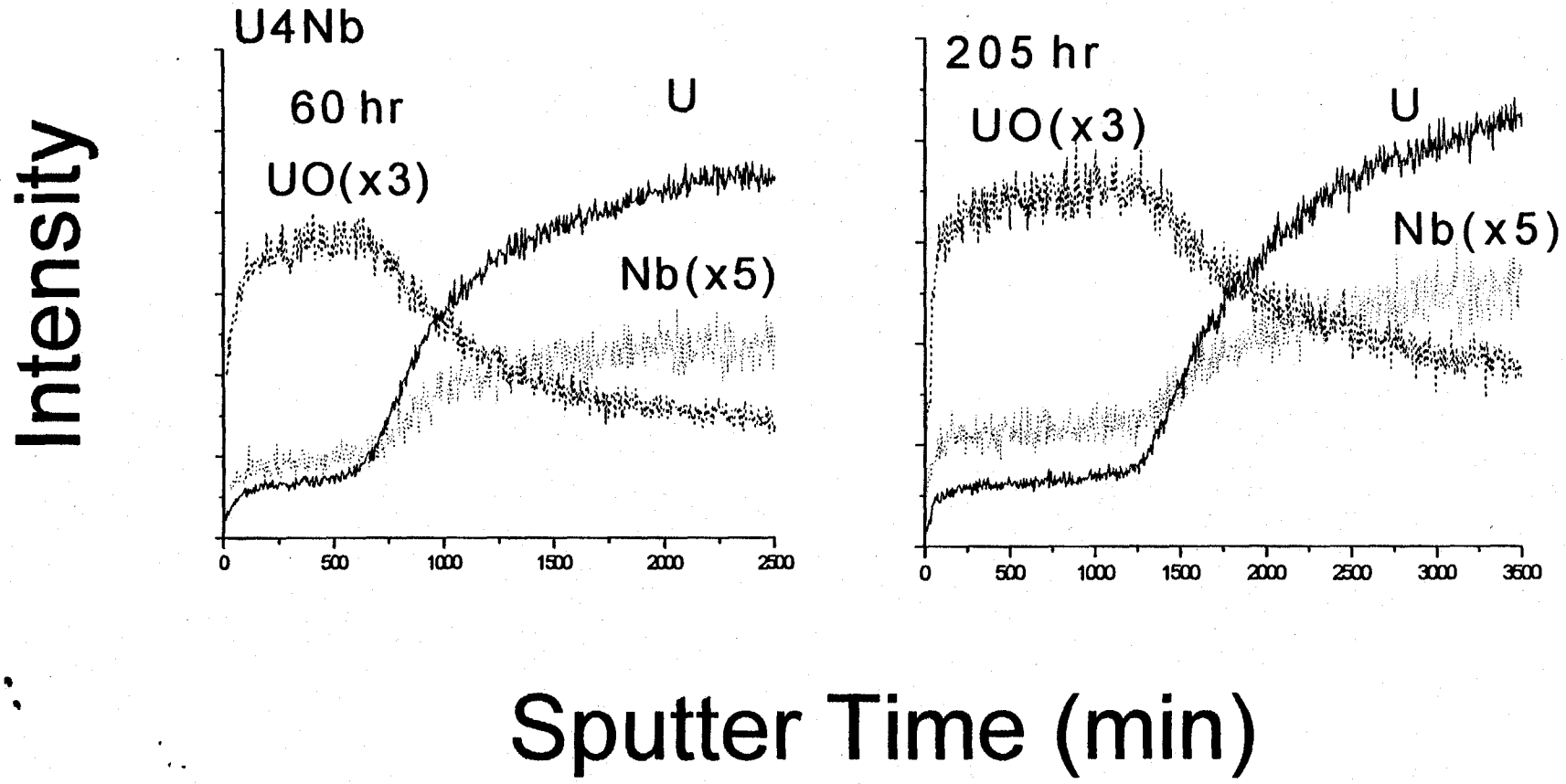
U4Nb
60 hr
UO(x3)
U
Nb(x5)
0
500
1000
1500
2000
2500
205 hr
UO(x3)
U
Nb(x5)
0
500
1000
1500
2000
2500
3000
3500
Intensity
Sputter Time (min)

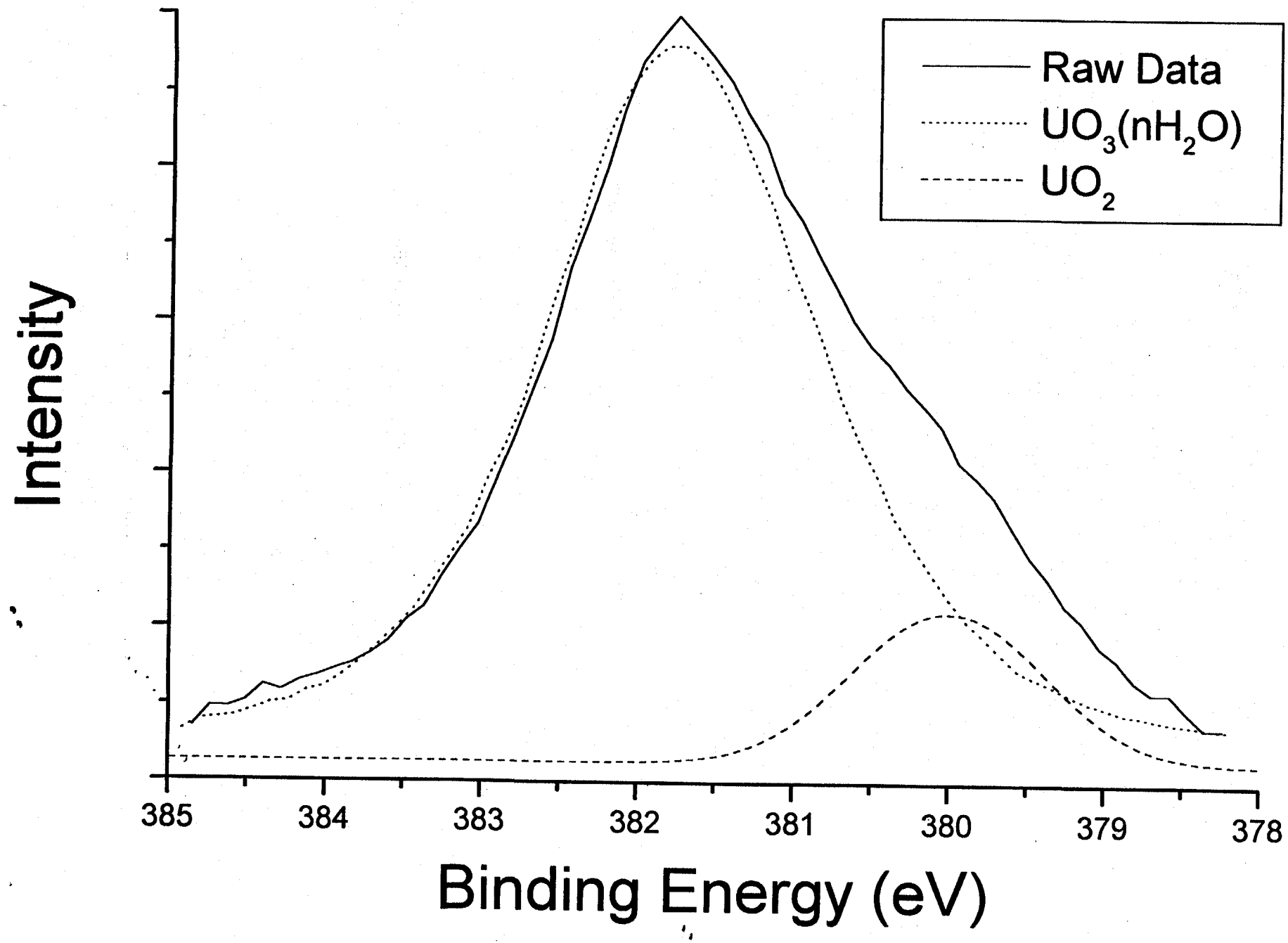
Raw Data
$UO_3(nH_2O)$
UO_2
Intensity
385
384
383
382
381
380
379
378
Binding Energy (eV)

FIG. 3

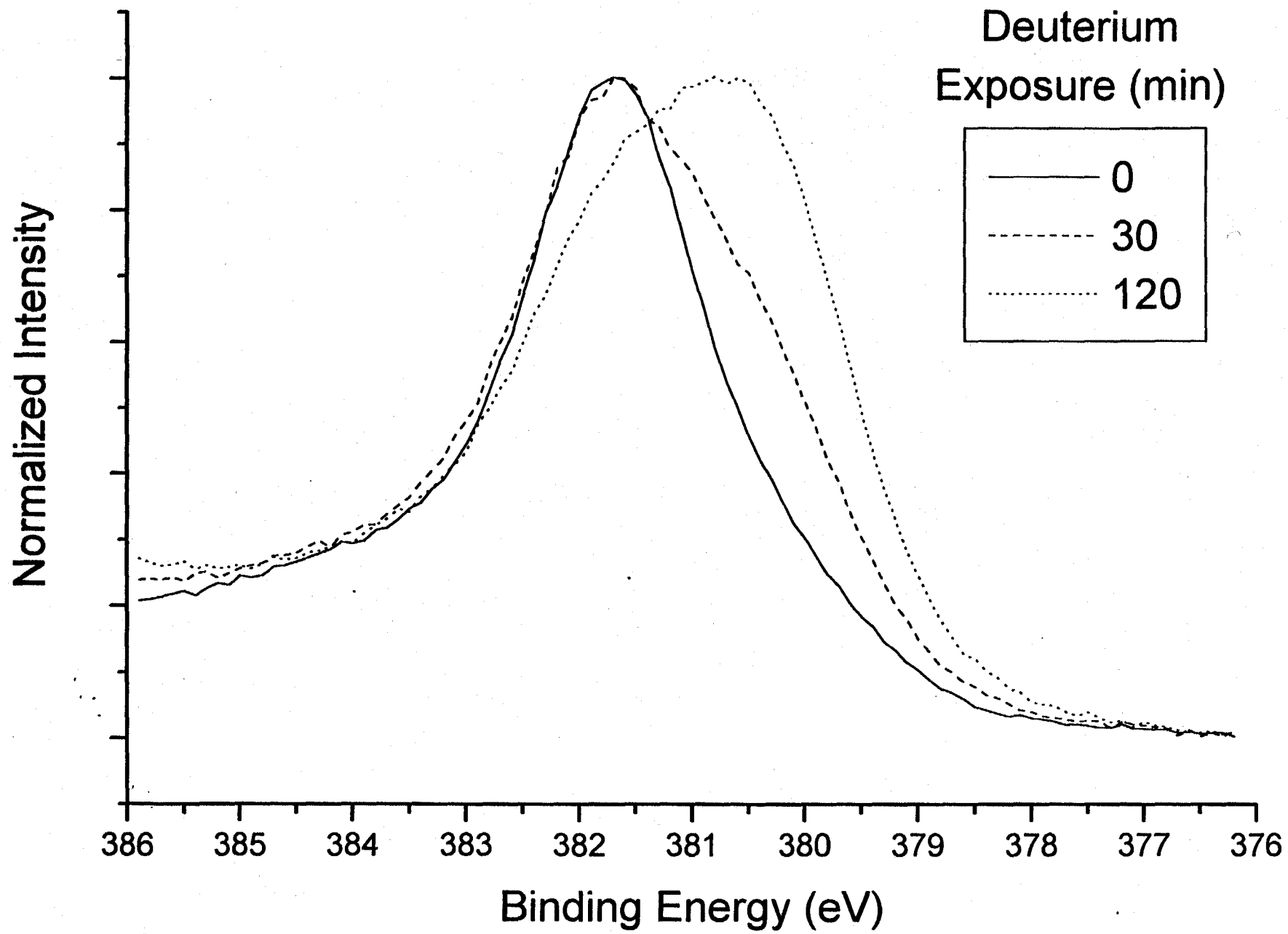
Deuterium
Exposure (min)
0
30
120
Normalized Intensity
386
385
384
383
382
381
380
379
378
377
376
Binding Energy (eV)

FIG 4